

Cosmological magnetic field correlators from blazar induced cascade

Hiroyuki Tashiro and Tanmay Vachaspati

Physics Department, Arizona State University, Tempe, Arizona 85287, USA.

(Dated: March 28, 2018)

TeV blazars offer an exciting prospect for discovering cosmological magnetic fields and for probing high energy processes, including CP violation, in the early universe. We propose a method for reconstructing both the non-helical and the helical magnetic field correlators using observations of cascade photons from TeV blazars.

I. INTRODUCTION

Large-scale magnetic fields with micro Gauss strength have been observed in galaxies [1, 2] and clusters of galaxies [3, 4]. Although it is assumed that such magnetic fields are the result of amplification from weak seed magnetic fields, the origin of the seed magnetic field has not yet been understood. There are two classes of models for the seed generation mechanism: astrophysical and cosmological models. In astrophysical models, the seeds are associated with nonlinear structures, and are generated during structure formation through the Biermann battery effect [5], or the Weibel instability [6]. On the other hand, seeds in the cosmological models are produced in the early universe and exist as extragalactic magnetic fields. This class of models includes the generation mechanisms in an inflationary epoch, during cosmological phase transitions, and at the epoch of recombination (for recent reviews, see [7–9]).

Recent gamma ray observations suggest the existence of cosmological magnetic fields stronger than $\sim 10^{-16}$ Gauss in the voids [10–12]. Although more detailed work will be required to establish this lower limit [13–15], the suggestion of such magnetic fields in large-scale structure voids, ~ 100 Mpc away from non-linear structures, provides a strong argument in favor of cosmological models. Further support in favor of an early universe origin can be obtained if the cosmological galactic magnetic fields are “helical”, thus indicating a process of magneto-genesis that fundamentally violates invariance under charge conjugation plus parity reflection (CP) [16].

Magnetic helicity density is defined as

$$h = \frac{1}{V} \int_V d^3x \mathbf{A} \cdot \mathbf{B}, \quad (1)$$

where \mathbf{A} is the vector potential of magnetic fields \mathbf{B} with $\mathbf{B} = \nabla \times \mathbf{A}$. Magnetic helicity is odd under CP transformations as \mathbf{A} and \mathbf{B} are odd under C, while \mathbf{A} is even but \mathbf{B} is odd under P. Non-zero magnetic helicity is predicted in scenarios in which cosmic baryogenesis and magneto-genesis occur concurrently during a cosmological phase transition [16–20]. Then the magnetic helicity density is related to the cosmic baryon number density and the CP violation responsible for the excess of matter over antimatter also provides helicity to the magnetic field. Other scenarios that can generate helical magnetic fields that are not tied to baryogenesis have been studied in Refs. [21–23]. Helicity is also an important factor in the evolution of magnetic fields because it helps to transfer magnetic field energy from small to large length scales, a process called an “inverse cascade”. Due to the inverse cascade, helical magnetic fields can grow to astrophysically relevant scales at the present epoch, even though the initial scale of the magnetic field extends only up to the much smaller cosmological horizon scale at the time of the phase transition.

The two point correlator of a stochastic, homogeneous, isotropic magnetic field contains two independent functions. In physical space, these are the normal and helical correlation functions ($M_N(r)$ and $M_H(r)$); in momentum space, these are the symmetric and antisymmetric power spectra ($S(k)$ and $A(k)$). There are several tools to measure the normal correlator (or the symmetric power spectrum) of cosmological magnetic fields but measuring helicity directly is more challenging. The detection of helicity of cosmological magnetic fields has been a primary motivation for this work, as few other direct schemes to detect helicity have been proposed [24].

A measurement of the normal correlator itself, together with some theoretical input, provides indirect access to the helicity of the magnetic field. This is because the presence of helicity influences the evolution of the normal correlator, and the exponents characterizing the normal correlator can give us some information about the magnetic helicity (for the evolution in the cosmological context, see Ref.[25–30]). The shape of the normal correlator, in particular the existence of a peak in the distribution can also inform us about the epoch of magneto-genesis. If magnetic fields are produced during inflation, the symmetric power spectrum can be expected to be scale invariant with significant power on the present day horizon scale.

Direct measures of the helical power spectrum are more difficult. For *astrophysical* magnetic helicity, it has been suggested that the correlation between Faraday rotation measurement and the polarization degree of radio synchrotron emission [31–33] can be used. For *cosmological* magnetic helicity, Ref. [24] has shown that correlations in the arrival momenta of very high energy cosmic rays are sensitive to the intervening magnetic helicity provided the cosmic ray

source locations are known. Cosmic Microwave Background (CMB) anisotropy observations may also permit a measure of the helicity through non-vanishing cross-correlation between the temperature and B-mode polarization anisotropies and between the E-mode and B-mode polarization anisotropies [34–36].

In the present paper, we propose a scheme to measure both the normal and the helical correlation functions of cosmological magnetic fields by using TeV blazar observations. Gamma rays with energy greater than ~ 1 TeV can scatter with ambient “extragalactic background light” (EBL) photons to pair produce electrons and positrons. The generated electrons and positrons create a secondary cascade of GeV gamma rays through the Inverse Compton (IC) scattering of CMB photons. As the electron and positron trajectories are bent due to the Lorentz force by a magnetic field, the GeV photon cascade carries information about the structure of the cosmological magnetic field. We show that cross-correlations between the arrival directions of the secondary cascade gamma rays at different energies are related to the correlation function of the extragalactic magnetic fields. If we imagine the cascade photon arrival direction to be a vector in the plane of observation, the inner product of vectors at different energies gives the normal part of the magnetic field correlation, and the outer product gives the helical correlator.

In Sec. II we describe the basic geometry of the process and evaluate the arrival direction of cascade photons as a function of the intervening magnetic field. In Sec. III we evaluate correlators of the arrival directions of cascade photons and relate them to the magnetic field correlation functions. Our results are placed in the context of observations in Sec. IV where we discuss estimators for the theoretical correlation functions we have found in Sec. III. Our analysis uses many simplifying assumptions that we discuss together with conclusions in Sec. V. Throughout this paper, we use natural units: $\hbar = 1 = c$.

II. GEOMETRICAL SETUP AND DEFLECTION ANGLE

TeV gamma rays from distant sources at redshift z_s cannot propagate freely over cosmological distances because, at such energies, interaction with the EBL can produce electrons and positrons. The mean free path of a gamma ray with energy E_{TeV} is given by [37]

$$D_{\text{TeV}}(E_{\text{TeV}}) \sim 80 \frac{\kappa}{(1+z_s)^2} \text{Mpc} \left(\frac{E_{\text{TeV}}}{10 \text{ TeV}} \right)^{-1}, \quad (2)$$

where κ is a numerical factor which accounts for the model uncertainties of EBL. Here we take $\kappa \sim 1$ [37]. Electrons and positrons generated by the TeV gamma ray lose energy by the production of a secondary gamma ray cascade through the IC scattering of CMB photons, and have a mean free path,

$$D_e \sim 30 \text{ kpc} (1+z_e)^{-4} \left(\frac{E_e}{10 \text{ TeV}} \right)^{-1}, \quad (3)$$

where z_e is the typical redshift at which TeV gamma rays create pairs, and $E_e \sim E_{\text{TeV}}/2$ is the electron energy. The up-scattered CMB photon has energy,

$$E_\gamma = \frac{4}{3} (1+z_e)^{-1} \epsilon_{\text{CMB}} \left(\frac{E_e}{m_e} \right)^2 \sim 88 \text{ GeV} \left(\frac{E_{\text{TeV}}}{10 \text{ TeV}} \right)^2, \quad (4)$$

where $\epsilon_{\text{CMB}} = 6 \times 10^{-4} (1+z_e)$ eV is the typical energy of CMB photons. Therefore we observe cascade gamma rays with energy $\sim E_\gamma$, in addition to TeV gamma rays with energy $\sim E_{\text{TeV}}$.

It is believed that TeV gamma rays are beamed from distant blazars in a narrow jet of opening angle $\theta_j \sim 5^\circ [\Gamma/10]^{-1}$ where Γ is the Lorentz factor of the gamma ray emitting plasma. The highest energy photons are observed if we lie within the opening angle of the jet. Denoting the angle between the source direction and the jet axis by θ_o , we require $\theta_o < \theta_j$. As emphasized in Ref. [38], the most likely situation is that we are located on the edge of the cone, as depicted in Fig. 1.

Suppose that the blazar is located at $\mathbf{x}_s = D_s \hat{\mathbf{n}}_s$ in the observer frame. We will assume for simplicity that the redshift of the source is less than one and take $1+z_s \sim 1$. If there are no magnetic fields in the IGM, we will observe cascade gamma rays due to TeV gamma rays also in the direction $\hat{\mathbf{n}}_s$. However if cosmological magnetic fields are present, the cascade gamma rays arrive from different directions. We now evaluate the arrival direction assuming a stochastic, homogeneous, and isotropic magnetic field.

Consider an observed cascade gamma ray that resulted from a TeV gamma ray with energy E_{TeV} that was emitted at $t = 0$ at an angle θ_e from the line of sight as depicted in Fig. 1. The TeV gamma ray produces an electron at the position \mathbf{x}_i at time $t = t_i$, where $t_i = D_{\text{TeV}}$. The produced electron has momentum \mathbf{P}_i whose amplitude P_i

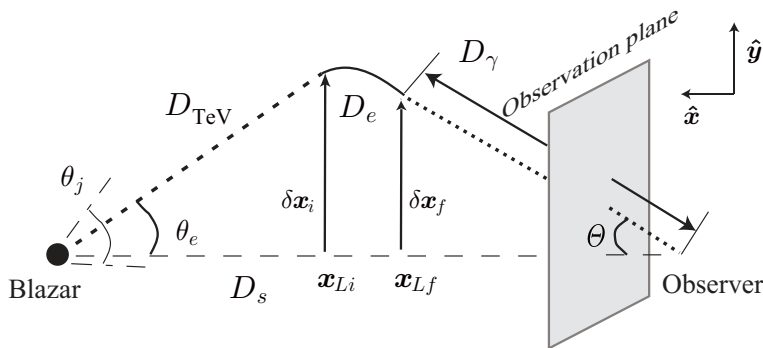


FIG. 1. The blazar on the left beams TeV photons within a jet of opening angle θ_j . The observer is most likely located at the edge of the jet, not on the axis. TeV photons pair produce after propagating a distance D_{TeV} . The pairs are bent by ambient magnetic fields and up-scatter CMB photons that propagate a distance D_γ to the observer. The emission angle θ_e , the observation direction Θ , the distance to the source D_s , and the pair creation and IC scattering event positions, $(x_{Li}, \delta x_i)$, $(x_{Lf}, \delta x_f)$ are also shown.

corresponds to the energy $E_e \approx E_{\text{TeV}}/2$. Since the opening angle of the electron-positron pair is very small, of order $m_e/E_e \sim 10^{-7}$, the direction \mathbf{P}_i is the same as the direction of the initial TeV gamma ray.

The momentum of the electron changes on propagation due to the Lorentz force,

$$\mathbf{P}(t) = \mathbf{P}_i + q \int_{t_i}^t dt' \mathbf{v}(t') \times \mathbf{B}(\mathbf{x}(t')) \quad (5)$$

where $q = \pm e$ is the electron/positron charge, $\mathbf{x}(t)$ and $\mathbf{v}(t)$ are the position and velocity of the electron (or positron), namely $\mathbf{v}(t) = \dot{\mathbf{x}}(t)$ where the overdot denotes differentiation with respect to time. (For convenience, from now on we shall refer to the charged particle as being the electron.)

We will now decompose all vectors in components parallel and perpendicular to the source direction. For example, the momentum and the position of the electron at time t is decomposed as

$$\mathbf{P}(t) = \mathbf{P}_L(t) + \delta \mathbf{p}(t), \quad \mathbf{x}(t) = \mathbf{x}_L(t) + \delta \mathbf{x}(t), \quad (6)$$

where the subscript L means the component parallel to the source direction (line-of-sight for TeV source). Therefore, the vector $\delta \mathbf{p}(t)$ and $\delta \mathbf{x}(t)$ are the deviations induced by the magnetic field.

In terms of the decomposed components, Eq. (5) can be written as

$$\mathbf{P}_L(t) + \delta \mathbf{p}(t) = \mathbf{P}_{Li} + \delta \mathbf{p}_i + q \int_{t_i}^t dt' [\mathbf{v}_L(t') + \delta \mathbf{v}(t')] \times \mathbf{B}(\mathbf{x}(t')), \quad (7)$$

where \mathbf{P}_{Li} and $\delta \mathbf{p}_i$ are the momentum components at time $t = t_i$. Note that at this stage, instead of replacing \mathbf{x} by \mathbf{x}_L in the argument of \mathbf{B} , we perform the integration along the actual path $\mathbf{x}(t)$. This is important if the magnetic fields have significant power on small scales, *i.e.*, a blue spectrum.

The bending angle of the electron is estimated as $\delta = D_e/R_L \sim 1.2 \times 10^{-3} [B/10^{-16} \text{ G}][E_{\text{TeV}}/10 \text{ TeV}]^{-2}$ where $R_L = E_e/qB$ is the Larmor radius. Here we have assumed a magnetic field coherence scale larger than D_e ; otherwise the electron trajectory would be diffusive yielding a smaller estimate for δ . Then the maximum deviation from the source direction is $\delta x_i \sim 90 \text{ kpc} (1 - D_{\text{TeV}}/D_s) [B/10^{-16} \text{ G}][E_{\text{TeV}}/10 \text{ TeV}]^{-3}$. Since the bending angle is small, we can treat $\delta \mathbf{p}$, $\delta \mathbf{x}$ and $\delta \mathbf{v}$ as perturbations. To linear order in the magnetic field strength, Eq. (7) becomes

$$\delta \mathbf{p}(t) = \delta \mathbf{p}_i + q \int_{t_i}^t dt' \mathbf{v}_L(t') \times \mathbf{B}(\mathbf{x}(t')). \quad (8)$$

The electron energy E_e is constant during this process, since a magnetic field does no work. Dividing Eq. (8) by E_e , we obtain the velocity,

$$\delta \mathbf{v}(t) = \delta \mathbf{v}_i + \frac{q}{E_e} \int_{t_i}^t dt' \mathbf{v}_L(t') \times \mathbf{B}(\mathbf{x}(t')), \quad (9)$$

and another integration gives the trajectory,

$$\delta\mathbf{x}(t) - \delta\mathbf{x}_i = \delta\mathbf{v}_i(t - t_i) + \frac{q}{E_e} \int_{t_i}^t dt'' \int_{t_i}^{t''} dt' \mathbf{v}_L(t') \times \mathbf{B}(\mathbf{x}(t')). \quad (10)$$

At any point in the electron's trajectory there is a probability of an IC scattering event with a CMB photon. We simplify the present analysis by assuming that the electron travels a fixed distance $D_e(E_e)$, and at final time t_f up-scatters a CMB photon. Since the electron is ultra-relativistic with Lorentz boost factor $E_e/m_e \sim 10^7$, the cascade gamma ray propagates along the momentum of the electron. Therefore the arrival direction of the cascade gamma ray is the same as the direction of the position $\mathbf{x}_f = \mathbf{x}(t_f)$.

We now define the vector Θ in the observation plane by

$$\Theta \equiv \frac{\delta\mathbf{x}_i - \delta\mathbf{x}_f}{D_e} \quad (11)$$

where $\delta\mathbf{x}_f$ is $\delta\mathbf{x}(t)$ at $t = t_f$. The magnitude, $|\Theta|$, is the observed angle Θ shown in Fig. 1, and the direction in the observation plane corresponds to the azimuthal direction of the original TeV gamma ray.

We will now relate Θ to the magnetic field using Eq. (10). However $\delta\mathbf{v}_i$ is still unknown in Eq. (10). To evaluate it, we first need to express the emission angle θ_e in terms of the observed angle Θ . Applying the trigonometric law of sines to the triangle formed by the source, observer and electron position – recall that $D_e \ll D_s$ – we obtain

$$\theta_e \approx \frac{D_\gamma}{D_{\text{TeV}}} \Theta \approx \frac{D_s - D_{\text{TeV}}}{D_{\text{TeV}}} \Theta. \quad (12)$$

In terms of Θ , the vector $\delta\mathbf{v}_i$ can now be written as

$$\delta\mathbf{v}_i = v_e \theta_e \hat{\mathbf{y}} = v_e \frac{D_s - D_{\text{TeV}}}{D_{\text{TeV}}} \Theta, \quad (13)$$

where v_e is the magnitude of the electron velocity, and $\hat{\mathbf{y}}$ is the unit vector perpendicular to the line-of-sight (see Fig. 1).

Now Eqs. (10), (11) and (13) give,

$$\Theta(E_\gamma) = -\frac{qD_{\text{TeV}}}{E_e D_e D_s} \int_{t_i}^{t_f} dt'' \int_{t_i}^{t''} dt' \mathbf{v}_L(t') \times \mathbf{B}(\mathbf{x}(t')), \quad (14)$$

where we can rewrite D_{TeV} , D_e , and E_e as functions of E_γ ,

$$D_{\text{TeV}}(E_{\text{TeV}}) \sim 80 \text{ Mpc} \left(\frac{E_\gamma}{88 \text{ GeV}} \right)^{-1/2}, \quad (15)$$

$$D_e \sim 30 \text{ kpc} \left(\frac{E_\gamma}{88 \text{ GeV}} \right)^{-1/2}, \quad (16)$$

$$E_e \sim 10 \text{ TeV} \left(\frac{E_\gamma}{88 \text{ GeV}} \right)^{1/2}. \quad (17)$$

With these relations, the magnitude of $\Theta(E_\gamma)$ is roughly estimated as

$$\Theta(E_\gamma) \approx \frac{qD_{\text{TeV}}D_e}{E_e D_s} v_L B \approx 7.3 \times 10^{-5} \left(\frac{B}{10^{-16} \text{ Gauss}} \right) \left(\frac{E_\gamma}{100 \text{ GeV}} \right)^{-3/2} \left(\frac{D_s}{1000 \text{ Mpc}} \right)^{-1}. \quad (18)$$

III. CORRELATORS AND PREDICTIONS

The vector $\Theta(E_\gamma)$ describes the position of the observed cascade gamma ray in the observation plane but its magnitude depends on geometrical factors such as the distance to the source (Eq. (14)). We define a rescaled vector to remove such dependence,

$$\mathbf{Q}(E_\gamma) \equiv \frac{E_e D_s}{q D_{\text{TeV}} D_e} \Theta(E_\gamma). \quad (19)$$

Now we are interested in two types of correlators of the $\mathbf{Q}(E_\gamma)$ vectors

$$F(E_1, E_2) = \langle \mathbf{Q}(E_1) \cdot \mathbf{Q}(E_2) \rangle, \quad (20)$$

$$G(E_1, E_2) = \langle \mathbf{Q}(E_1) \times \mathbf{Q}(E_2) \cdot \hat{\mathbf{x}} \rangle, \quad (21)$$

where E_1 and E_2 are two energies of the observed cascade gamma rays, and we recall that we have set up our coordinate system so that the x -axis is along the line of sight, *i.e.*, $\hat{\mathbf{x}}$ is normal to the observation plane.

The ensemble value $\langle Q_i(E_1)Q_{i'}(E_2) \rangle$, where i and i' denote components in the observation plane, can be written by using the magnetic field correlation function, Eq. (14),

$$\langle Q_i(E_1)Q_{i'}(E_2) \rangle = \epsilon_{ijl}\epsilon_{i'j'l'}v_L^j(E_1)v_L^{j'}(E_2) \int_{t_{1i}}^{t_{1f}} \frac{dt'_1}{D_{e1}} \int_{t_{1i}}^{t'_1} \frac{dt_1}{D_{e1}} \int_{t_{2i}}^{t_{2f}} \frac{dt'_2}{D_{e2}} \int_{t_i}^{t'_2} \frac{dt_2}{D_{e2}} \langle B^l(\mathbf{x}(t_1, E_1))B^{l'}(\mathbf{x}(t_2, E_2)) \rangle, \quad (22)$$

where D_{e1} and D_{e2} are D_e for the cascade gamma ray with energy E_1 and E_2 respectively. Note that the velocity $\mathbf{v}_L = (1, 0, 0)$ and $t_f - t_i = D_e$.

The correlation function of a stochastic, homogeneous, and isotropic magnetic field is given by [39]

$$\langle B_i(\mathbf{x} + \mathbf{r})B_j(\mathbf{x}) \rangle = M_N(r) \left[\delta_{ij} - \frac{r_i r_j}{r^2} \right] + M_L(r) \frac{r_i r_j}{r^2} + M_H(r) \epsilon_{ijl} r^l, \quad (23)$$

where $M_N(r)$, $M_L(r)$, and $M_H(r)$ are the correlation functions for the normal, longitudinal, and helical parts of the magnetic fields. Due to the homogeneity and isotropy of the magnetic fields, these correlations depend only on the separation distance $r = |\mathbf{r}|$. The divergence-less condition gives

$$M_N(r) = \frac{1}{2r} \frac{d}{dr} (r^2 M_L(r)). \quad (24)$$

The stochastic fields are often described by power spectra in Fourier space. The magnetic field correlation function in Fourier space is

$$\langle \tilde{B}_i^*(\mathbf{k}) \tilde{B}_j(\mathbf{k}') \rangle = (2\pi)^3 \delta^3(\mathbf{k} - \mathbf{k}') \left[\left(\delta_{ij} - \frac{k_i k_j}{k^2} \right) S(k) + i \epsilon_{ijl} \frac{k_l}{k} A(k) \right], \quad (25)$$

where $S(k)$ and $A(k)$ are the symmetric and antisymmetric (helical) parts of the magnetic field power spectrum. The functions $S(k)$ and $A(k)$ are related to the correlation functions $M_N(r)$, $M_L(r)$, and $M_H(r)$ as in [39].

Therefore the ensemble average, Eq. (22), can also be decomposed into three parts: the normal, longitudinal, and helical parts,

$$\langle Q_i(E_1)Q_{i'}(E_2) \rangle = C_{Nii'} + C_{Lii'} + C_{Hii'}. \quad (26)$$

with each of the terms given by four integrations as in Eq. (22). The separation scale, r , appearing in the correlators $M_N(r)$, $M_L(r)$ and $M_H(r)$ is the magnitude of the separation vector

$$\mathbf{r}(t_1, t_2, E_1, E_2) \equiv \mathbf{x}(t_1, E_1) - \mathbf{x}(t_2, E_2). \quad (27)$$

Since cosmological magnetic fields are weak, this can be approximated as

$$\mathbf{r}(t_1, t_2, E_1, E_2) \approx \mathbf{x}_L(t_1, E_1) - \mathbf{x}_L(t_2, E_2). \quad (28)$$

Therefore,

$$\mathbf{r}(t_1, t_2, E_1, E_2) = (D_{\text{TeV}}(E_1) - D_{\text{TeV}}(E_2) + (t_1 - t_{1i}) - (t_2 - t_{2i})) \hat{\mathbf{x}}. \quad (29)$$

For $t_1 = t_{1f}$ and $t_2 = t_{2f}$, the separation scale becomes

$$r(t_{1f}, t_{2f}, E_1, E_2) = D_{\text{TeV}}(E_1) - D_{\text{TeV}}(E_2) + D_e(E_1) - D_e(E_2). \quad (30)$$

In the case with $i = i' \neq x$, C_{Lii} and C_{Hii} vanish, because only the $\hat{\mathbf{x}}$ components of \mathbf{v}_L and \mathbf{r} are non-vanishing. However the normal correlator does not vanish and C_{Nii} is given by

$$C_{Nii}(E_1, E_2) = \int_{t_{1i}}^{t_{1f}} dt'_1 \int_{t_{1i}}^{t'_1} dt_1 \int_{t_{2i}}^{t_{2f}} dt'_2 \int_{t_i}^{t'_2} dt_2 M_N(r(t_1, t_2, E_1, E_2)). \quad (31)$$

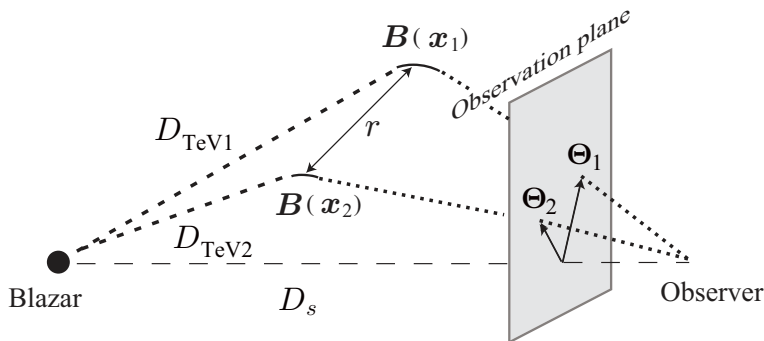


FIG. 2. Events at two different energies sample the magnetic field in regions of size $D_e \sim 30$ kpc (solid lines at the vertices of the triangles). The regions themselves are separated by distance r which can be ~ 100 Mpc depending on the energy difference of the two events. Energy resolution of the detector translates into a lower limit on the separation at which the magnetic field correlations can be probed.

In the case with $i \neq i'$, $i \neq x$ and $i' \neq x$, while $C_{Nii'}$ and $C_{Lii'}$ vanish, $C_{Hii'}$ has non-zero value,

$$C_{Hii'} = \epsilon_{ii'z} \int_{t_{1i}}^{t_{1f}} dt'_1 \int_{t_{1i}}^{t'_1} dt_1 \int_{t_{2i}}^{t_{2f}} dt'_2 \int_{t_{2i}}^{t'_2} dt_2 M_H(r(t_1, t_2, E_1, E_2))(\mathbf{r}(t_1, t_2, E_1, E_2) \cdot \hat{\mathbf{x}}), \quad (32)$$

Therefore F and G can be written directly in terms of the magnetic field correlation functions,

$$F(E_1, E_2) = 2 \int_{t_{1i}}^{t_{1f}} \frac{dt'_1}{D_{e1}} \int_{t_{1i}}^{t'_1} \frac{dt_1}{D_{e1}} \int_{t_{2i}}^{t_{2f}} \frac{dt'_2}{D_{e2}} \int_{t_{2i}}^{t'_2} \frac{dt_2}{D_{e2}} M_N(r(t_1, t_2, E_1, E_2)), \quad (33)$$

$$G(E_1, E_2) = 2 \int_{t_{1i}}^{t_{1f}} \frac{dt'_1}{D_{e1}} \int_{t_{1i}}^{t'_1} \frac{dt_1}{D_{e1}} \int_{t_{2i}}^{t_{2f}} \frac{dt'_2}{D_{e2}} \int_{t_{2i}}^{t'_2} \frac{dt_2}{D_{e2}} M_H(r(t_1, t_2, E_1, E_2))(\mathbf{r}(t_1, t_2, E_1, E_2) \cdot \hat{\mathbf{x}}). \quad (34)$$

It is worth pointing out that $F(E_\gamma, E_\gamma) \neq 0$ but $G(E_\gamma, E_\gamma) = 0$.

We have already seen that $D_{\text{TeV}} \gg D_e$ independently of E_γ , and so the separation scale in the magnetic field correlation function can be approximated as,

$$r(t_1, t_2, E_1, E_2) \approx D_{\text{TeV}}(E_1) - D_{\text{TeV}}(E_2). \quad (35)$$

Then recalling $t_f - t_i = D_e$, we can do the integrations in Eqs. (33) and (34) to get

$$F(E_1, E_2) \approx \frac{1}{2} M_N(|r_{12}|), \quad (36)$$

$$G(E_1, E_2) \approx \frac{1}{2} M_H(|r_{12}|) r_{12}, \quad (37)$$

where r_{12} is $r_{12} = D_{\text{TeV}}(E_1) - D_{\text{TeV}}(E_2)$. This shows that we can obtain both the non-helical and the helical magnetic field correlation functions through the correlators $F(E_1, E_2)$ and $G(E_1, E_2)$ constructed from the arrival information of cascade photons. This is the main result of this paper.

Note, as shown in Fig. 2, that the obtained correlator is on the scale r_{12} which can be much larger than the scale D_e . This is because the magnetic field gets correlated at the spatial points where pair production occurs and these can be separated by hundreds of Mpc depending on the values chosen for E_1 and E_2 . It remains an interesting open question if further refinements of the above method can lead to correlators on scales smaller than $D_e \sim 30$ kpc.

IV. OBSERVATIONS AND ESTIMATORS

In the previous section, we have considered correlators in the arrival directions of cascade photons and expressed them in terms of correlators of the intervening magnetic field. In this section we consider the problem of determining

magnetic field correlators from the observers point of view: given cascade arrival direction data, what quantity should be calculated that corresponds to the magnetic field correlator? The calculated quantity will at best be an estimator for the magnetic field correlator because observations are limited in number, while the magnetic field correlator in Eq. (23) is over an infinite ensemble of realizations.

In a more realistic setting – see simulations in Ref. [40] – observed gamma rays with some energy E are expected to be scattered around a typical observation direction on the observational plane. The scattering is due to differences in the magnetic field along the trajectories of different electrons and also the stochasticity of the EBL and CMB photons. We have not considered the latter fluctuations in this paper but the variation in the magnetic field can be smoothed out by taking the average $\langle \Theta(E) \rangle$ over all observed gamma rays with the same energy E . Even if the magnetic fields have small-scale structure, *i.e.*, a blue spectrum, the averaging procedure should yield the correct magnetic field correlator on scales larger than the smoothing scale, $|\delta \mathbf{x}| \sim 90$ kpc.

There is a second way to smooth out fluctuations in the magnetic field. This is by realizing that the correlation functions $F(E_1, E_2)$ and $G(E_1, E_2)$ evaluated in the previous section depend on only one function, $r(t_1, t_2, E_1, E_2)$. Hence there are many choices of E_1 and E_2 yielding the same r , and one of the energy variables can be integrated out. This corresponds to averaging over all pairs of energies such that the distance r remains fixed (see Fig. 2). Using Eq. (35) we see that $r(t_1, t_2, E_\gamma, E_\gamma + \delta E)$ is independent of E_γ provided

$$\delta E(E_\gamma, r) = 27 \text{ GeV} \left[\left(\frac{r}{10 \text{ Mpc}} - \sqrt{\frac{88 \text{ GeV}}{E_\gamma}} \right)^{-2} - \frac{88 \text{ GeV}}{E_\gamma} \right]. \quad (38)$$

We can now average Eqs. (36) and (37) over E_1 while taking $E_2 = E_1 + \delta E$,

$$M_N(r) \approx 2 \int \frac{dE_\gamma}{\Delta E} \mathbf{Q}(E_\gamma) \cdot \mathbf{Q}(E_\gamma + \delta E(E_\gamma, r)), \quad (39)$$

$$rM_H(r) \approx 2 \int \frac{dE_\gamma}{\Delta E} \mathbf{Q}(E_\gamma) \times \mathbf{Q}(E_\gamma + \delta E(E_\gamma, r)) \cdot \hat{\mathbf{x}}, \quad (40)$$

where ΔE is the integration range of the observation energy. The vector $\mathbf{Q}(E)$ now denotes the *average* (rescaled) direction vector for cascade photons with energy E .

A third way to perform the ensemble average is to use observations of many TeV blazars because cascade gamma rays from different blazars sample magnetic fields along different path. Hence we can obtain the magnetic field correlation function using

$$M_N(r) \approx \frac{2}{N} \sum_\alpha \left[2 \int \frac{dE_\gamma}{\Delta E} \mathbf{Q}(E_\gamma) \cdot \mathbf{Q}(E_\gamma + \delta E(E_\gamma, r)) \right]_\alpha, \quad (41)$$

$$rM_H(r) \approx \frac{2}{N} \sum_\alpha \left[2 \int \frac{dE_\gamma}{\Delta E} \mathbf{Q}(E_\gamma) \times \mathbf{Q}(E_\gamma + \delta E(E_\gamma, r)) \cdot \hat{\mathbf{x}} \right]_\alpha, \quad (42)$$

where α labels the blazar.

Finally we would like to remark that the most likely observation of a TeV blazar is when we are positioned at the edge of the jet [38], but we are even more likely to be located outside the jet opening angle. Then we will not observe the TeV source but will still receive some cascade GeV photons. In this case, if there is reason to suppose that the observed photons are indeed from a cascade, we can extend our correlator by replacing $\mathbf{Q}(E)$ in Eqs. (41), (42) by $\mathbf{Q}(E) - \mathbf{Q}(E_*)$ where E_* is the highest energy (and least deviated) cascade photon that is observed. We can still draw some conclusions about the magnetic field correlators though the analysis is more involved.

V. DISCUSSION AND CONCLUSIONS

Our main result is the connection between cosmological magnetic field correlators and the correlators of cascade photons as given in Eqs. (36) and (37) together with the definitions in Eqs. (20) and (21). In the observational context, this connection can be written as in Eqs. (41) and (42). These relations suggest that observations of cascade photons may be used to directly study the non-helical and helical spectra of cosmological magnetic fields. There are few other

direct ways to probe the helicity of cosmological magnetic fields and this is an important feature of the technique we have described.

Our analysis will need further development as it has used many simplifying assumptions. For example, the stochastic interactions of the TeV photons with the EBL photons will lead to a probability distribution for D_{TeV} while we have used a fixed value. Similarly there will be probability distributions for the other interactions, and the magnetic field will have some structure on small scales. In addition, if the blazar is at high redshift, cosmological expansion will become important. These effects can best be studied using Monte Carlo simulations similar to the ones described in Refs. [40, 41]. The simulations should be able to confirm if the magnetic field correlators can be recovered from realistic data, which hopefully will become available in the near future.

ACKNOWLEDGMENTS

We thank Nat Butler and Francesc Ferrer for discussion. This work was supported by the DOE at ASU.

-
- [1] P. P. Kronberg, J. J. Perry, & E. L. H. Zukowski, *Astrophys. J.* **387**, 528 (1992).
 - [2] M. L. Bernet, F. Miniati, S. J. Lilly, P. P. Kronberg and M. Dessauges-Zavadsky, *Nature* **454**, 302 (2008) [[arXiv:0807.3347](#) [astro-ph]].
 - [3] T. E. Clarke, P. P. Kronberg and H. Boehringer, *Astrophys. J.* **547**, L111 (2001) [[astro-ph/0011281](#)].
 - [4] A. Bonafede, L. Feretti, M. Murgia, F. Govoni, G. Giovannini, D. Dallacasa, K. Dolag and G. B. Taylor, *A&A* **513**, A30 (2010) [[arXiv:1002.0594](#) [astro-ph.CO]].
 - [5] P. L. Biermann and C. F. Galea, “The Early Universe and the Cosmic Microwave Background: Theory and Observations” Proceedings of the NATO Advanced Study Institute, (2003) [[astro-ph/0302168](#)].
 - [6] M. Lazar, R. Schlickeiser, R. Wielebinski, S. Poedts, *Astrophys. J.* **693**, 1133, 2009
 - [7] A. Kandus, K. E. Kunze and C. G. Tsagas, *Phys. Rept.* **505**, 1 (2011) [[arXiv:1007.3891](#) [astro-ph.CO]].
 - [8] L. M. Widrow, D. Ryu, D. R. G. Schleicher, K. Subramanian, C. G. Tsagas and R. A. Treumann, *Space Sci. Rev.* **166**, 37 (2012) [[arXiv:1109.4052](#) [astro-ph.CO]].
 - [9] R. Durrer and A. Neronov, [[arXiv:1303.7121](#) [astro-ph.CO]].
 - [10] A. Neronov, I. Vovk and , *Science* **328**, 73 (2010) [[arXiv:1006.3504](#) [astro-ph.HE]].
 - [11] F. Tavecchio, G. Ghisellini, L. Foschini, G. Bonnoli, G. Ghirlanda and P. Coppi, *Mon. Not. Roy. Astron. Soc.* **406**, L70 (2010) [[arXiv:1004.1329](#) [astro-ph.CO]].
 - [12] K. Dolag, M. Kachelriess, S. Ostapchenko and R. Tomas, *Astrophys. J.* **727**, L4 (2011) [[arXiv:1009.1782](#) [astro-ph.HE]].
 - [13] A. E. Broderick, P. Chang and C. Pfrommer, *Astrophys. J.* **752**, 22 (2012) [[arXiv:1106.5494](#) [astro-ph.CO]].
 - [14] F. Miniati and A. Elyiv, [[arXiv:1208.1761](#) [astro-ph.CO]].
 - [15] R. Schlickeiser R., D. Ibscher, M. Supsar, *Astrophys. J.* **758**, 102 (2012).
 - [16] T. Vachaspati, *Phys. Rev. Lett.* **87**, 251302 (2001) [[astro-ph/0101261](#)].
 - [17] T. Vachaspati, *Phys. Lett. B* **265**, 258 (1991).
 - [18] M. Joyce and M. E. Shaposhnikov, *Phys. Rev. Lett.* **79**, 1193 (1997) [[astro-ph/9703005](#)].
 - [19] J. M. Cornwall, *Phys. Rev. D* **56**, 6146 (1997) [[hep-th/9704022](#)].
 - [20] H. Tashiro, T. Vachaspati and A. Vilenkin, *Phys. Rev. D* **86**, 105033 (2012) [[arXiv:1206.5549](#) [astro-ph.CO]].
 - [21] G. B. Field and S. M. Carroll, *Phys. Rev. D* **62**, 103008 (2000) [[astro-ph/9811206](#)].
 - [22] L. Campanelli and M. Giannotti, *Phys. Rev. D* **72**, 123001 (2005) [[astro-ph/0508653](#)].
 - [23] L. Campanelli, *Int. J. Mod. Phys. D* **18**, 1395 (2009) [[arXiv:0805.0575](#) [astro-ph]].
 - [24] T. Kahniashvili and T. Vachaspati, *Phys. Rev. D* **73**, 063507 (2006) [[astro-ph/0511373](#)].
 - [25] M. Christensson, M. Hindmarsh and A. Brandenburg, *Astron. Nachr.* **326**, 393 (2005) [[astro-ph/0209119](#)].
 - [26] L. Campanelli, *Phys. Rev. D* **70**, 083009 (2004) [[astro-ph/0407056](#)].
 - [27] R. Banerjee and K. Jedamzik, *Phys. Rev. D* **70**, 123003 (2004) [[astro-ph/0410032](#)].
 - [28] L. Campanelli, *Phys. Rev. Lett.* **98**, 251302 (2007) [[arXiv:0705.2308](#) [astro-ph]].
 - [29] A. Boyarsky, J. Frohlich and O. Ruchayskiy, *Phys. Rev. Lett.* **108**, 031301 (2012) [[arXiv:1109.3350](#) [astro-ph.CO]].
 - [30] T. Kahniashvili, A. G. Tevzadze, A. Brandenburg and A. Neronov, [[arXiv:1212.0596](#) [astro-ph.CO]].
 - [31] A. A. Volegova, R. A. Stepanov, *JETPL*, 90, 637 (2010)
 - [32] H. Junklewitz and T. A. Ensslin, *A&A* **530**, A88 (2011) [[arXiv:1008.1243](#) [astro-ph.IM]].
 - [33] N. Oppermann, H. Junklewitz, G. Robbers and T. A. Ensslin, *A&A*, 530, A89 (2011). [[arXiv:1008.1246](#) [astro-ph.IM]].
 - [34] C. Caprini, R. Durrer and T. Kahniashvili, *Phys. Rev. D* **69**, 063006 (2004) [[astro-ph/0304556](#)].
 - [35] T. Kahniashvili and B. Ratra, *Phys. Rev. D* **71**, 103006 (2005) [[astro-ph/0503709](#)].
 - [36] K. E. Kunze, *Phys. Rev. D* **85**, 083004 (2012) [[arXiv:1112.4797](#) [astro-ph.CO]].
 - [37] A. Neronov and D. V. Semikoz, *Phys. Rev. D* **80**, 123012 (2009) [[arXiv:0910.1920](#) [astro-ph.CO]].
 - [38] C. M. Urry and P. Padovani, M. Stickel, *Astrophys. J.* **382**, 501 (1991)

- [39] Monin A. S., Iaglom A. M., Statistical fluid mechanics: Mechanics of turbulence. Volume 2, Cambridge, Mass., MIT Press, (1975).
- [40] A. Elyiv, A. Neronov and D. V. Semikoz, Phys. Rev. D **80**, 023010 (2009) [[arXiv:0903.3649](#) [astro-ph.CO]].
- [41] K. Dolag, M. Kachelriess, S. Ostapchenko and R. Tomas, Astrophys. J. **703**, 1078 (2009) [[arXiv:0903.2842](#) [astro-ph.HE]].